

Selective D2 receptor PET in manganese-exposed workers

Susan R. Criswell, MD, Mark N. Warden, MS, Susan Searles Nielsen, PhD, Joel S. Perlmutter, MD, Stephen M. Moerlein, PharmD, PhD, Lianne Sheppard, PhD, Jason Lenox-Krug, MS, Harvey Checkoway, PhD, and Brad A. Racette, MD

Correspondence

Dr. Racette
racetteb@wustl.edu

Neurology® 2018;91:e1022-e1030. doi:10.1212/WNL.0000000000006163

Abstract

Objective

To investigate the associations between manganese (Mn) exposure, D2 dopamine receptors (D2Rs), and parkinsonism using [¹¹C](N-methyl)benperidol (NMB) PET.

Methods

We used NMB PET to evaluate 50 workers with a range of Mn exposure: 22 Mn-exposed welders, 15 Mn-exposed workers, and 13 nonexposed workers. Cumulative Mn exposure was estimated from work histories, and movement disorder specialists examined all workers. We calculated NMB D2R nondisplaceable binding potential (BPND) for the striatum, globus pallidus, thalamus, and substantia nigra (SN). Multivariate analysis of covariance with post hoc descriptive discriminant analysis identified regional differences by exposure group. We used linear regression to examine the association among Mn exposure, Unified Parkinson's Disease Rating Scale motor subsection 3 (UPDRS3) score, and regional D2R BPND.

Results

D2R BPND in the SN had the greatest discriminant power among exposure groups ($p < 0.01$). Age-adjusted SN D2R BPND was 0.073 (95% confidence interval [CI] 0.022–0.124) greater in Mn-exposed welders and 0.068 (95% CI 0.013–0.124) greater in Mn-exposed workers compared to nonexposed workers. After adjustment for age, SN D2R BPND was 0.0021 (95% CI 0.0005–0.0042) higher for each year of Mn exposure. Each 0.10 increase in SN D2R BPND was associated with a 2.65 (95% CI 0.56–4.75) increase in UPDRS3 score.

Conclusions and relevance

Nigral D2R BPND increased with Mn exposure and clinical parkinsonism, indicating dose-dependent dopaminergic dysfunction of the SN in Mn neurotoxicity.

From the Department of Neurology (S.R.C., M.N.W., S.S.N., J.S.P., J.L.-K., B.A.R.), Department of Radiology (J.S.P., S.M.M.), Department of Neuroscience (J.S.P.), Program in Physical Therapy (J.S.P.), Program in Occupational Therapy (J.S.P.), and Department of Biochemistry and Molecular Biophysics (S.M.M.), Washington University School of Medicine, St. Louis, MO; Department of Environmental and Occupational Health Sciences (L.S.) and Department of Biostatistics (L.S.), University of Washington, School of Public Health, Seattle; Department of Family Medicine and Public Health (H.C.) and Department of Neurosciences (H.C.), University of California, San Diego, School of Medicine, La Jolla; and School of Public Health (B.A.R.), Faculty of Health Sciences, University of the Witwatersrand, Parktown, South Africa.

Go to Neurology.org/N for full disclosures. Funding information and disclosures deemed relevant by the authors, if any, are provided at the end of the article.

Glossary

AIC = Akaike information criterion; **AP** = anterior putamen; **BPND** = nondisplaceable binding potential; **CI** = confidence interval; **D2R** = D2 dopamine receptor; **GP** = globus pallidus; **MPRAGE** = magnetization-prepared rapid gradient echo; **NMB** = [¹¹C](N-methyl)benperidol; **PD** = Parkinson disease; **PI** = pallidal index; **PP** = posterior putamen; **SN** = substantia nigra; **3D** = 3-dimensional; **UPDRS3** = Unified Parkinson's Disease Rating Scale motor subsection 3; **VOI** = volume of interest.

In excess, manganese (Mn) is a neurotoxicant that targets basal ganglia,¹ but understanding of the pathogenic mechanisms in humans remains limited. Alterations of striatal and extrastriatal D2 dopamine receptor (D2R) concentrations have been implicated in the pathophysiology of movement disorders, including parkinsonism² and dystonia,^{3,4} both of which can be seen in Mn neurotoxicity. D2Rs are expressed presynaptically on dopaminergic neurons and postsynaptically on dopaminergic neuronal pathways throughout the brain.⁵⁻⁷ The functional roles of D2Rs are complex with their diffuse distribution and dual presynaptic and postsynaptic expression.^{6,8,9}

PET permits in vivo assessment of dopamine receptors, although previous studies with D2R PET ligands in human and nonhuman primate models of Mn toxicity used nonspecific PET radioligands for the D2R family with similar affinity for D2R and D3 receptor subtypes.^{3,10,11} Competition from endogenous dopamine may alter brain uptake and retention of these radioligands¹²⁻¹⁴ and may have contributed to inconsistent results across studies.¹⁵⁻¹⁹

The PET radioligand [¹¹C](N-methyl)benperidol (NMB) is an analog of the dopamine receptor antagonist benperidol and has both high affinity and selectivity for D2R but is not displaced by endogenous dopamine.^{3,20} In the present study, we evaluated the relationship between occupational Mn exposure, D2R density, and parkinsonism using NMB PET imaging in Mn-exposed workers and nonexposed workers, clinically characterized by a movement disorder specialist. We hypothesized that Mn exposure would be associated with dose-dependent differences in D2R density indicating dopaminergic dysfunction.

Methods

Standard protocol approvals, registrations, and patient consents

This study was approved by the Washington University Human Research Protection Office and the Radioactive Drug Research Committee, and all participants provided written informed consent.

Participants

All participants (n = 50) were workers from the US Midwest and were recruited from May 2013 to September 2016. To obtain a range of Mn exposures, we recruited from 2 sources. Some (n = 32) were International Brotherhood of Boilermakers union members who participated in a previous cohort study²¹ of Mn-exposed workers. The remainder (n = 18) were workers

engaged in construction who were recruited from a carpentry union. The study was designed to have 90% power to detect a 10% difference in NMB binding between groups. In total, 22 workers conducted welding (welders or welder helpers, hereafter called Mn-exposed welders), 15 workers who worked around welding fume (hereafter called Mn-exposed workers), and 13 workers who were not occupationally exposed to Mn. Inclusion criteria were no history of stroke, brain tumor, or other condition that could compromise the Unified Parkinson's Disease Rating Scale motor subsection 3 (UPDRS3) score²²; no antiparkinsonian medications, neuroleptics, or amphetamines; and age ≥18 years, as detailed previously.²¹ We excluded 2 workers due to medical conditions on the basis of these criteria. Covariate data were available for all workers.

Clinical assessment

A movement disorders specialist blinded to Mn exposure examined all workers and rated them using the UPDRS3. The 2 examiners in this study each rated 10 videos of patients with Parkinson disease (PD) each year, and the intraclass correlation coefficient for UPDRS3 ratings was >90%. However, to account for potential differences by examiner overall and by study time, we adjusted UPDRS3 scores as previously described.²¹

MRI acquisition

We acquired high resolution 3-dimensional (3D) magnetization-prepared rapid gradient echo (MPRAGE) images on each worker using a Siemens 3T Magnetom Trio or Prisma scanner (Erlangen, Germany) (repetition time = 2,400 milliseconds, inversion time = 1,000 milliseconds, echo time = 3.14 milliseconds, flip angle = 8°, 0.9 × 0.9 × 0.9-mm voxels). Cumulative Mn exposure is associated with increased globus pallidus (GP) T1 signal, and the signal intensity is traditionally measured in terms of a pallidal index (PI), defined as the ratio of T1 signal in the GP to a white matter reference region.^{23,24} PIs were calculated from the MPRAGE images as previously described²³: $PI = ([\text{left GP} + \text{right GP}] / [\text{left control region} + \text{right control region}]) \times 100$.

PET acquisition

NMB was synthesized as previously described.²⁵ A single Siemens/CTI EXACT+ scanner, which has 32 rings of bismuth germanate detector elements and acquires 63 simultaneous slices with 2.4-mm spacing and an axial field of view of 15.5 cm, was used to acquire scans in 3D mode. Three retractable germanium 68 (⁶⁸Ge) rod sources were used for transmission scans to measure individual attenuation factors. Transaxial and axial spatial resolution at slice center are 4.3- and 4.1-mm full width half-maximum in 3D mode.²⁶ NMB (5–25.67 mCi) was injected IV into an arm vein over 20 seconds. Dynamic PET images were

obtained for 120 minutes beginning with radioligand injection, with three 1-minute frames followed by four 2-minute frames, three 3-minute frames, and 20 five-minute frames. PET scans were reconstructed with filtered back-projection with ramp filter cutoff at the Nyquist frequency and included attenuation, scatter, and random correction.

Image analysis

For each worker, we coregistered dynamically acquired PET image frames to each other and to the individual's MPRAGE image using methods previously outlined.⁷ A priori MRI-defined volumes of interest (VOIs) included caudate, anterior and posterior putamen (AP and PP), GP, thalamus, substantia nigra (SN), a standard white matter reference region for the MRI PI, and a cerebellar reference region for the NMB PET. We used FreeSurfer²⁷ for segmentation of the subcortical deep nuclei and cerebellum on individual MRIs. Caudate, AP, PP, GP, thalamus, and cerebellum were identified with FreeSurfer, and a single investigator manually edited these volumes. The cerebellar volume included all gray and white matter from both hemispheres. The putamen VOIs were manually separated at the posterior fornix on individual MPRAGEs as defined previously.²³ The SN and white matter reference regions were manually traced following previously published methods.^{23,28} All VOIs were reviewed by an independent second investigator. We eroded VOIs to minimize partial volume effects on the regional PET measurements of radioactivity. For the caudate, AP, PP, GP, and thalamus, we combined a gaussian smoothing filter at a 3-mm full width half-maximum with thresholding set to 0.75 to erode the surface of the original region. The SN VOI was not large enough to erode.

For each worker, the FreeSurfer-defined VOIs and reference region were resampled in Talairach atlas space²⁹ to 3 mm, and decay-corrected tissue activity curves were extracted from the dynamic PET data.³⁰ D2R nondisplaceable binding potential (BPND) was calculated for each VOI with the Logan graphical method³¹ with cerebellum as the reference region. Slopes were obtained from Logan plot points for data acquired 60 to 120 minutes after NMB injection. Left and right BPNDs were averaged for all VOIs. We checked for potential variations in PET scanning over time and found no evidence of association between D2R BPND and scan date.

Exposure assessment

All workers completed or updated a validated, structured questionnaire in person at the time of imaging, which included a detailed work history.³² From this, we created categorical Mn exposure groups based on intensity of welding fume exposure as described above. We also calculated 2 cumulative Mn exposure variables, the total years of welding fume exposure and mg Mn/m³-years.²¹ The latter variable takes into account both duration (years) and intensity (mg Mn/m³) of exposure. All exposure variables were available for all participants.

Statistical analysis

We used R version 3.3.1 with the DiscrMiner package³³ for all statistical analyses. We verified that the VOI D2R BPNDs were

multivariate normally distributed and performed multivariate analysis of covariance³⁴ as an omnibus test to determine whether differences existed among the exposure groups, covarying with age and using the Pillai trace as the test statistic. We used post hoc descriptive discriminate analysis³⁴ to determine which VOIs drove any group differences and corrected this analysis for 6 multiple comparisons using the Benjamini-Hochberg procedure³⁵ with the false discovery rate set at 0.10. Finally, for VOIs with the greatest discriminate power, we used multivariable linear regression to examine associations within each VOI between D2R BPND and exposure and D2R BPND and examiner-adjusted UPDRS3 score as continuous measures. We verified linearity by residual analysis and locally weighted scatterplot smoothing.³⁶ When locally weighted scatterplot smoothing suggested a possible alternative model, we compared it to the linear model using Akaike information criterion (AIC).³⁷ We examined influential points defined by a Cook distance $>4/(\text{number of participants} - \text{number of predictors} - 1)$ as a measure of the leverage of a data point on the model.³⁸ In addition to the full models, we performed models with influential points excluded, in case these points distorted the association because of sample size. Parameter significance tests were 2 sided in all models.

We adjusted for age, centered at 43 years (median age among nonexposed), in all models unless noted because age may influence D2R BPND.²⁵ We compared exposure groups to the nonexposed workers on key demographics using pairwise *t* tests. We repeated all analyses restricted to men and examined the effects of volume size on D2R BPND. There was no association between volume and D2R BPND for the SN, AP, or thalamus; however, there were significant linear associations between volume and D2R BPND for the caudate, GP, and PP, so we performed a sensitivity analysis adjusting for volume in these VOIs. We explored the associations in clinically normal workers (UPDRS3 score ≤ 6) because inclusion of Mn-exposed workers with nonnormal UPDRS3 scores might enhance the association between D2R BPND and exposure. For this sensitivity analysis, we compared nonexposed workers with the Mn-exposed participants as a single group ($n = 12$). There were 2 participants with a first-degree family history of PD. We repeated all analyses excluding these 2 workers.

Data availability

Data from research participants in this study, who authorized sharing of their research data, will be made available to investigators with appropriate expertise and research support after publication of the primary aims of this study. All shared data will be deidentified and will be released in accordance with US regulations.

Results

Subject characteristics

Most workers were non-Hispanic white men (table 1). The exposure groups were similar in terms of sex and age. Both

Mn-exposed workers and welders had relatively wide ranges of Mn exposure. The age-adjusted PI was higher in Mn-exposed workers (5.2 points, $p = 0.10$) and Mn-exposed welders (6.0 points, $p = 0.04$) than nonexposed workers. Similarly, UPDRS3 scores were higher in both Mn-exposed workers (mean 6.9, $p \leq 0.01$) and welders (mean 11.3, $p \leq 0.01$) compared to the nonexposed workers (mean 2.1). The

most common parkinsonian features in the Mn-exposed participants were limb bradykinesia, axial signs, and limb rigidity. Action tremor was markedly more prevalent than rest tremor (table 1). No workers had a diagnosis of PD or received any treatment for parkinsonism, including chelation. As previously reported, these workers had $\approx 12\%$ lower 6- ^{18}F fluoro-L-dopa uptake in the caudate nucleus.^{23,39}

Table 1 Characteristics of participating workers by welding fume exposure

Characteristics	Mn-exposed welders (n = 22)	Mn-exposed workers (n = 15)	Nonexposed reference workers (n = 13)
Male, n (%)	20 (91)	14 (93)	12 (92)
Non-Hispanic white, n (%)	21 (95)	14 (93)	12 (92)
Age, y			
Mean (SD)	47.7 (12.3)	48.8 (12.3)	44.8 (10.3)
Median	46	50	43
Range	27–67	23–69	29–64
Welding fume exposure, y			
Mean (SD)	24.0 (14.2)	16.3 (12.8)	0 (0)
Median	20.1	13.5	0
Range	3.1–47.5	0.1–47.1	0–0
mg Mn/m³-year^a			
Mean (SD)	2.6 (2.0)	0.3 (0.2)	0 (0)
Median	1.8	0.2	0
Range	0.4–6.6	0.001–0.8	0–0
MRI pallidal index			
Mean (SD)	123.5 (11.4)	122.7 (5.3)	117.5 (5.3)
Median	122.7	123.2	119.7
Range	105.6–151.4	109.4–129.6	107.3–123.5
UPDRS3 score			
Mean (SD)	11.3 (6.2)	6.9 (5.6)	2.1 (1.6)
Median	11.75	5.5	2.0
Range	1–23	0.5–19	0–6
UPDRS3 score ≤ 6 , n (%)	4 (18)	8 (53)	13 (100)
Signs of parkinsonism (mean, SD)^b			
Limb bradykinesia	5.70 (3.90)	3.83 (3.61)	1.70 (1.44)
Limb rigidity	3.14 (2.51)	1.33 (1.85)	0 (0)
Action tremor	0.32 (0.65)	0.53 (0.90)	0 (0)
Rest tremor	0 (0)	0.17 (0.52)	0 (0)
Axial signs ^c	2.14 (1.48)	1 (1.07)	0.38 (0.51)

Abbreviation: UPDRS3 = Unified Parkinson's Disease Rating Scale motor subsection 3.

^a Based on weighted welding years as described previously multiplied by 0.14.²¹

^b Derived from UPDRS3.

^c Axial signs include gait, posture, postural stability, arising from a chair, global bradykinesia, neck rigidity, expression, and speech.

Mn exposure intensity and NMB PET

Multivariate analysis of covariance demonstrated differences in D2R BPNDs among the 3 exposure groups while covarying for age (Pillai trace = 0.45, $p = 0.04$). Post hoc descriptive discriminant analysis revealed that the SN ($p < 0.01$) and caudate ($p = 0.09$) had the greatest discriminant power. The SN remained significant after correction for multiple comparisons. Linear regression demonstrated that SN D2R BPND was higher in both Mn-exposed workers and Mn-exposed welders compared to nonexposed workers (all $p \leq 0.05$, table 2 and figure 1). When restricted to workers who had UPDRS3 scores ≤ 6 , SN D2R BPND uptake remained similarly higher (0.07,

95% confidence interval [CI] 0.01–0.13) in Mn-exposed ($n = 12$) compared to nonexposed workers ($n = 13$) ($p = 0.02$) (data not shown in tables). We also re-examined the difference between exposure groups while adjusting for caudate, GP, and PP volume and found no substantial changes. Similarly, results did not change with the analysis limited to men or excluding the 2 workers with a family history of PD in a first-degree relative.

Cumulative Mn exposure and NMB PET

SN D2R BPND increased with all cumulative Mn exposure measures, with and without influential points (all $p \leq 0.09$, table 3). The association between duration in an Mn-exposed job

Table 2 Mean D2R receptor NMB BPND by brain volume and Mn exposure group ($n = 50$)

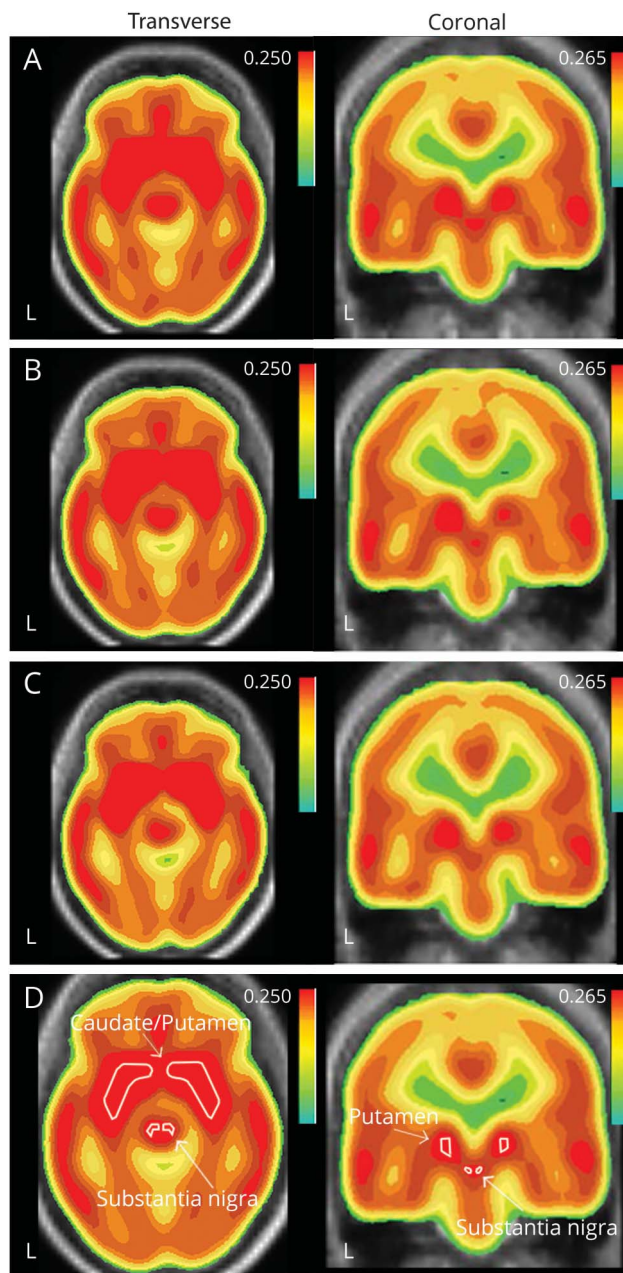
Brain volume	Unadjusted		Age adjusted	
	Mean	Difference from nonexposed (95% CI)	Mean	Difference from nonexposed (95% CI)
Caudate				
Nonexposed workers	1.7238	Reference	1.7512	Reference
Mn-exposed workers	1.6127	-0.111 (-0.324 to 0.102)	1.7025	-0.049 (-0.212 to 0.115)
Mn-exposed welders	1.8225	0.099 (-0.097 to 0.295)	1.8950	0.144 (-0.007 to 0.294) ^a
Anterior putamen				
Nonexposed workers	2.4782	Reference	2.5023	Reference
Mn-exposed workers	2.4205	-0.057 (-0.274 to 0.160)	2.4997	-0.003 (-0.186 to 0.181)
Mn-exposed welders	2.4435	-0.035 (-0.236 to 0.166)	2.5075	0.005 (-0.164 to 0.174)
Posterior putamen				
Nonexposed workers	2.1264	Reference	2.1522	Reference
Mn-exposed workers	2.0761	-0.050 (-0.273 to 0.290)	2.0761	0.009 (-0.175 to 0.192)
Mn-exposed welders	2.1163	-0.010 (-0.216 to 0.196)	2.1163	0.032 (-0.137 to 0.201)
Thalamus				
Nonexposed workers	0.3989	Reference	0.3975	Reference
Mn-exposed workers	0.4047	0.006 (-0.043 to 0.055)	0.4002	0.003 (-0.047 to 0.052)
Mn-exposed welders	0.4182	0.193 (-0.026 to 0.065)	0.4146	0.017 (-0.029 to 0.063)
Globus pallidus				
Nonexposed workers	1.9593	Reference	1.9711	Reference
Mn-exposed workers	1.9193	-0.040 (-0.309 to 0.229)	1.9583	-0.013 (-0.280 to 0.255)
Mn-exposed welders	1.9636	0.004 (-0.244 to 0.253)	1.9951	0.024 (-0.222 to 0.270)
Substantia nigra				
Nonexposed workers	0.1401	Reference	0.1381	Reference
Mn-exposed workers	0.2128	0.073 (0.018 to 0.128) ^b	0.2065	0.068 (0.013 to 0.124) ^b
Mn-exposed welders	0.2162	0.076 (0.025 to 0.127) ^b	0.2111	0.073 (0.022 to 0.123) ^b

Abbreviations: BPND = nondisplaceable binding potential; CI = confidence interval; D2R = D2 receptor; NMB = [¹¹C](N-methyl)benperidol.

^a $p < 0.10$.

^b $p < 0.05$.

Figure 1 Unadjusted composite [¹¹C](N-methyl)benperidol D2 receptor BPND by exposure group



(A) Mn-exposed welders, (B) Mn-exposed workers, (C) nonexposed reference workers in the striatum and midbrain overlaid on MRI in the transverse and coronal views, and (D) reference labels for the striatum and substantia nigra are provided for the composite image. However, volumes of interest for sampling are identified on individual MRI images as described in Methods. BPND = nondisplaceable binding potential.

and SN D2R BPND was clearly linear (figure 2A). For mg Mn/m³-years, which accounts for intensity and duration, it was unclear whether a linear model (AIC = -111.37, table 3) or a spline model (AIC = -112.86, table 3 and figure 2B) was superior. In the latter, the increase in SN D2R BPND was particularly marked in the lower range of exposure during the initial 0.8 mg Mn/m³-year.

NMB PET and UPDRS3

There was a linear association between SN D2R BPND and examiner-adjusted UPDRS3 score (2.84 increase in UPDRS3 score per 0.1 increase in nigral D2R BPND, 95% CI 0.55–5.14, $p = 0.02$) (figure 2C). This relationship persisted after adjustment for age (2.13 increase in UPDRS3 score per 0.1 increase in SN D2R BPND, 95% CI -0.03 to 4.29, $p = 0.05$) and was driven largely by the limb rigidity component of the UPDRS3 (1.21 increase in the limb rigidity subscore per 0.1 increase in nigral D2R BPND, 95% CI 0.39–2.02, $p \leq 0.01$). The exclusion of 1 influential point (young participant with a UPDRS3 score of >15) strengthened this relationship (2.65 increase per 0.1 increase in nigral D2R BPND, 95% CI 0.56–4.75, $p = 0.01$).

Discussion

In this large molecular imaging study of basal ganglia D2 receptors, we provide strong evidence that Mn-exposed welders and workers have higher SN D2R BPND than nonexposed workers using the D2R-specific tracer NMB. We also provide compelling evidence of a dose-response increase in SN D2R BPND with both cumulative Mn exposure and clinical parkinsonism. In contrast to previous smaller PET D2R studies in Mn-exposed human^{15,16} and nonhuman primate models of Mn neurotoxicity,^{17–19} we found similar to higher D2R density in the basal ganglia of Mn-exposed workers and welders relative to nonexposed workers. However, direct comparisons to these older studies are difficult because they included participants with advanced parkinsonism, used nonspecific D2/D3R tracers, and did not examine extrastriatal uptake.

This clear linear relationship between increasing SN D2R density and greater severity of parkinsonism as measured by the UPDRS3 strongly suggests that the SN is a target of Mn neurotoxicity. This association was largely driven by limb rigidity. This particular clinical sign was also a primary contributor to progression of parkinsonism related to welding fume exposure in our larger cohort.²¹ Taken together, these findings strongly suggest that limb rigidity may be a core clinical feature of Mn neurotoxicity. The specific relationship between SN D2R density and clinical parkinsonism has not been fully described. However, nonhuman primate studies demonstrate a strong correlation between increasing nigral dopaminergic cell loss and greater motor parkinsonism, whereas striatal changes in presynaptic dopaminergic neurons did not fully correlate with motor parkinsonism.^{40,41} In patients with PD, striatal D2R density may be higher than, lower than, or the same as in control participants, secondary to differences in disease severity and medication use.⁴² Increases in striatal D2R binding may represent compensatory upregulation of striatal D2Rs in early stages of PD, referred to as D2R denervation supersensitivity.⁴² However, with progressive degeneration of nigrostriatal pathways, striatal D2R binding decreases to normal or reduced levels

Table 3 Mn exposure and substantia nigra D2R BPND adjusted for age

	All workers (n = 50)		Excluding influential points ^a	
	Estimate (95% CI)	p Value	Estimate (95% CI)	p Value
mg Mn/m³-years, linear model^b				
Intercept	0.179 (0.152 to 0.205)	<0.0001 ^c	0.175 (0.151 to 0.199)	<0.0001 ^c
Per mg Mn/m ³ -year	0.0114 (-0.0019 to 0.025)	0.09	0.017 (0.004 to 0.029)	0.01 ^c
Age, per year	0.0006 (-0.001 to 0.003)	0.53	0.00002 (-0.002 to 0.002)	0.98
mg Mn/m³-years, spline model^d				
Intercept	0.160 (0.126 to 0.193)	<0.0001 ^c	0.159 (0.130 to 0.189)	<0.0001 ^c
Per mg Mn/m ³ -year ≤0.8	0.072 (-0.008 to 0.151)	0.08	0.088 (0.013 to 0.163)	0.02 ^c
Per mg Mn/m ³ -year >0.8	0.002 (-0.014 to 0.018)	0.78	0.0016 (-0.014 to 0.017)	0.84
Age, per year	0.0007 (-0.0013 to 0.0027)	0.49	0.00005 (-0.0019 to 0.0018)	0.97
Duration at Mn-exposed job, linear model^b				
Intercept	0.162 (0.131 to 0.193)	<0.0001 ^c	0.161 (0.127 to 0.184)	<0.0001 ^c
Per years at Mn-exposed job	0.0023 (0.0005 to 0.0042)	0.01 ^c	0.0026 (0.0008 to 0.0044)	0.005 ^c
Age, per year	-0.0005 (-0.0029 to 0.0018)	0.65	-0.0008 (-0.0030 to 0.0014)	0.44

Abbreviations: BPND = nondisplaceable binding potential; CI = confidence interval; D2R = D2 receptor.

^a Influential points had a Cook distance $>4/(n - p - 1)$, where n is the number of participants and p is the number of predictors in the model. Influential points are presented in figures as darkened markers. The number of influential points and which types of workers are influential differs by model, as footnoted, but never exceeded 4.

^b Two potentially influential points identified.

^c $p < 0.05$.

^d Four potentially influential points identified.

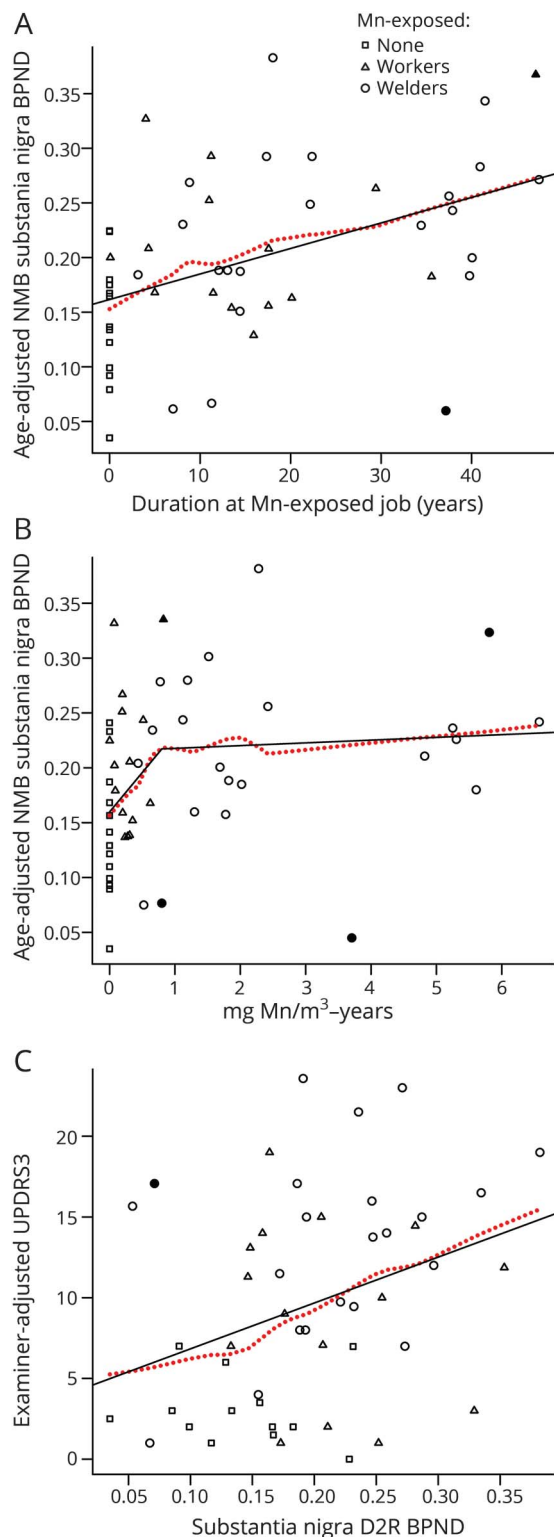
compared to healthy controls.^{43,44} Presynaptic D2R in the SN is located in the perikarya and dendrites of the pars compacta,⁶ which autoregulate dopamine release.^{45–47} Higher D2R NMB binding in the SN of Mn-exposed workers and welders could, therefore, represent a similar compensatory upregulation or may represent a direct effect of Mn exposure on SN D2Rs. Further exploration of these hypotheses will be an important area in future studies on the pathophysiology of Mn neurotoxicity.

We also demonstrated a dose-dependent increase in SN D2R BPND with all cumulative Mn exposure metrics. This included evidence for a linear association between both duration in an Mn-exposed jobs and Mn/m³-years and SN D2R BPND. Compared to the linear model, the Mn/m³-years spline model suggested an alternative interpretation that much of the change in SN D2R BPND occurs between 0 and 0.8 mg Mn/m³-year and increases only modestly thereafter. This suggests that there may be a critical Mn exposure window in the first 6 years of exposure. This is consistent with our recent longitudinal clinical cohort study in which we identified a particularly strong association between increasing welding fume exposure and progression of clinical parkinsonism in the first 5 years of exposure,²¹ although longitudinal imaging will be needed to determine whether Mn induces neurodegeneration of the dopaminergic system. Estimated mean time-weighted Mn exposure in

the present subset of the cohort was 0.11 to 0.14 mg Mn/m³ for Mn-exposed welders and 0.018 to 0.035 mg Mn/m³ for Mn-exposed workers and is representative of the overall cohort.²¹ These estimates are substantially lower than the US Occupational Safety and Health Administration Permissible Exposure Limit for Mn of 5 mg Mn/m³.⁴⁸ In contrast, the American Conference of Governmental Industrial Hygienists time-weighted average threshold limit value for inspirable Mn is 0.1 mg Mn/m³.⁴⁹ Given that we observe a linear relation between Mn exposure and SN D2R BPND in workers with estimated Mn exposures below these recommended exposure limits, our study provides additional support for reducing the Occupational Safety and Health Administration Permissible Exposure Limit to the American Conference of Governmental Industrial Hygienists threshold limit value or lower.

This study has several potential limitations. Welding fume contains a number of elements and gases⁵⁰; therefore, this study cannot fully exclude a contribution from other substances in welding fume, including iron, which competes for the same metal transporter responsible for Mn uptake into the brain.⁵¹ NMB PET is limited to the examination of D2R; therefore, we cannot exclude pathologic effects in other brain neurotransmitters. Similarly, while current evidence suggests that nigral D2Rs are located primarily in the SN pars compacta⁶ and that the SN pars reticulata is primarily

Figure 2 Associations between Mn exposure, NMB SN D2R BPND, and examiner-adjusted UPDRS3 (n = 50)



(A) Linear relationship between age-adjusted [¹¹C](N-methyl)benperidol (NMB) substantia nigra (SN) D2 dopamine receptor (D2R) nondisplaceable binding potential (BPND) and duration at an Mn-exposed job and (B) association with mg Mn/m³-years modeled with 2 linear splines with a knot at 0.8 mg Mn/m³-years. (C) There is also a linear relationship between NMB SN D2R BPND and examiner-adjusted Unified Parkinson's Disease Rating Scale motor subsection 3 (UPDRS3) score. Dotted line is the locally weighted scatterplot smoothing estimate; age-adjusted influential points based on the Cook distance are darkened.

populated by D1 receptors,⁴⁵ the presence of D2R within the pars reticulata or other nigral afferents cannot be excluded. Confirmation is required to understand the extent to which our findings in Mn-exposed workers translate to patients with PD. We also note that because all the workers were essentially of working age (not elderly) and we excluded workers taking dopaminergic medications (effectively excluding those diagnosed with PD), the only workers with a UPDRS3 score >6 were in the Mn-exposed groups. However, the consistency of our results in the sensitivity analysis, focusing only on workers with a UPDRS3 score ≤6, would argue against these criteria causing the difference in D2R BPND between the exposure groups. Finally, while we cannot fully exclude coexistent early PD, none of the workers was diagnosed with PD by the examining neurologist either at the time of imaging or during their participation in the larger cohort study (mean follow-up for Mn-exposed workers 4.3 years, for Mn-exposed welders 7.6 years), although the average age of these workers was substantially younger than the average age at PD onset. Once again, longitudinal evaluation is required to clarify whether the clinical and imaging phenotype we observed becomes consistent with PD.

Mn-exposed welders and workers demonstrated higher D2R-specific binding in the SN compared to nonexposed workers, suggesting nigral D2R upregulation. Furthermore, there was a dose-response linear increase in SN D2R BPND with greater Mn exposure, with much of the change occurring early in the course of welding exposure, suggesting that a critical exposure and intervention window may exist in the first 6 years of exposure. Finally, clinical parkinsonism increased linearly with greater SN D2R BPND, demonstrating nigral involvement in Mn-induced parkinsonism.

Author contributions

All authors had full access to all the data in the study and take responsibility for the integrity of the data and the accuracy of the data analysis. Study concept and design: Racette, Perlmutter, Criswell, Checkoway. Acquisition, analysis, or interpretation of data: all authors. Statistical analysis: Criswell, Warden, Nielsen, Sheppard. Drafting of the manuscript: Criswell, Warden, Nielsen, Lenox, Racette. Critical revision of the manuscript for important intellectual content: all authors. Obtained funding: Criswell, Racette. Administrative, technical, or material support: Moerlein, Lenox, Perlmutter. Supervision: Racette, Perlmutter.

Study funding

Funding for this project was provided by the following NIH grants: R01ES021488, K23ES021444, K24ES017765, R01ES013743, R01ES021488-02S1, P42ES004696, and ICTS UL1RR024992, as well as the American Parkinson Disease Association (APDA), and the Greater St. Louis Chapter of the APDA.

Disclosure

S. Criswell reports grant funding from the NIH, including K23ES021444 and R01ES013743. M. Warden reports no disclosures relevant to the manuscript. S. Searles Nielsen reports grant funding from the NIH, including K24ES017765 and R01ES021488, and grants from the Michael J. Fox Foundation and American Parkinson Disease Association. J. Perlmutter reports grant funding from the NIH, including R01ES021488 and R01ES013743. S. Moerlein reports grant funding from the NIH, including R01ES026187 and R01ES021488. J. Lenox-Krug reports no disclosures relevant to the manuscript. H. Checkoway reports grant funding from the NIH, including R01ES021488, R21ES026084, R01ES025991, and R01ES025792. B. Racette reports grant funding from NIH, including K24ES017765, R01ES021488, R01ES013743, P42ES004696, and UL1RR024992, as well as grant funding from APDA and the Michael J. Fox Foundation. Go to Neurology.org/N for full disclosures.

Received January 26, 2018. Accepted in final form June 15, 2018.

References

1. Parmelee NL, Aschner M. Manganese and aging. *Neurotoxicology* 2016;56:262–268.
2. Kaasinen V, Nagren K, Hietala J, et al. Extrastriatal dopamine D2 and D3 receptors in early and advanced Parkinson's disease. *Neurology* 2000;54:1482–1487.
3. Karimi M, Moerlein SM, Videen TO, et al. Decreased striatal dopamine receptor binding in primary focal dystonia: a D2 or D3 defect? *Mov Disord* 2011;26:100–106.
4. Perlmutter JS, Stambuk MK, Markham J, et al. Decreased [18F]spiperone binding in putamen in idiopathic focal dystonia. *J Neurosci* 1997;17:843–850.
5. Rankin J, Hazelwood LA, Free RB, Roof RA, Sibley DR. *Molecular Pharmacology of the Dopamine Receptors: Dopamine Handbook*. New York: Oxford Scholarship Online; 2010.
6. Missale C, Nash SR, Robinson SW, Jaber M, Caron MG. Dopamine receptors: from structure to function. *Physiol Rev* 1998;78:189–225.
7. Eisenstein SA, Koller JM, Piccirillo M, et al. Characterization of extrastriatal D2 in vivo specific binding of [(18) F](N-methyl)benperidol using PET. *Synapse* 2012;66:770–780.
8. Beaulieu JM, Gainetdinov RR. The physiology, signaling, and pharmacology of dopamine receptors. *Pharmacol Rev* 2011;63:182–217.
9. Sibley DR. New insights into dopaminergic receptor function using antisense and genetically altered animals. *Annu Rev Pharmacol Toxicol* 1999;39:313–341.
10. Elsinga PH, Hatano K, Ishiwata K. PET tracers for imaging of the dopaminergic system. *Curr Med Chem* 2006;13:2139–2153.
11. Halldin C, Farde L, Hogberg T, et al. Carbol-11-FLB 457: a radioligand for extrastriatal D2 dopamine receptors. *J Nucl Med* 1995;36:1275–1281.
12. Chou YH, Halldin C, Farde L. Effect of amphetamine on extrastriatal D2 dopamine receptor binding in the primate brain: a PET study. *Synapse* 2000;38:138–143.
13. Seeman P, Guan HC, Niznik HB. Endogenous dopamine lowers the dopamine D2 receptor density as measured by [3H]raclopride: implications for positron emission tomography of the human brain. *Synapse* 1989;3:96–97.
14. Cropley VL, Innis RB, Nathan PJ, et al. Small effect of dopamine release and no effect of dopamine depletion on [18F]fallypride binding in healthy humans. *Synapse* 2008;62:399–408.
15. Shinotoh H, Snow BJ, Chu NS, et al. Presynaptic and postsynaptic striatal dopaminergic function in patients with manganese intoxication: a positron emission tomography study. *Neurology* 1997;48:1053–1056.
16. Kessler KR, Wunderlich G, Hefter H, Seitz RJ. Secondary progressive chronic manganese associated with markedly decreased striatal D2 receptor density. *Mov Disord* 2003;18:217–218.
17. Shinotoh H, Snow BJ, Hewitt KA, et al. MRI and PET studies of manganese-intoxicated monkeys. *Neurology* 1995;45:1199–1204.
18. Eriksson H, Tedroff J, Thuomas KA, et al. Manganese induced brain lesions in Macaca fascicularis as revealed by positron emission tomography and magnetic resonance imaging. *Arch Toxicol* 1992;66:403–407.
19. Guilarte TR, Chen MK, McGlothan JL, et al. Nigrostriatal dopamine system dysfunction and subtle motor deficits in manganese-exposed non-human primates. *Exp Neurol* 2006;202:381–390.
20. Moerlein SM, Perlmutter JS, Markham J, Welch MJ. In vivo kinetics of [18F](N-methyl)benperidol: a novel PET tracer for assessment of dopaminergic D2-like receptor binding. *J Cereb Blood Flow Metab* 1997;17:833–845.
21. Racette BA, Searles Nielsen S, Criswell SR, et al. Dose-dependent progression of parkinsonism in manganese-exposed welders. *Neurology* 2017;88:344–351.

22. Fahn S, Elton RL; Members of the UPDRS Development Committee. Unified Parkinson's Disease Rating Scale. In: Fahn S, Marsden CD, Goldstein M, Calne DB, editors. *Recent Developments in Parkinson's Disease*, vol 2. Florham Park: Macmillan Health Care Information; 1987:153–163.
23. Criswell SR, Perlmutter JS, Videen TO, et al. Reduced uptake of [(18)F]FDOPA PET in asymptomatic welders with occupational manganese exposure. *Neurology* 2011;76:1296–1301.
24. Criswell SR, Perlmutter JS, Huang JL, et al. Basal ganglia intensity indices and diffusion weighted imaging in manganese-exposed welders. *Occup Environ Med* 2012;69:437–443.
25. Eisenstein SA, Antenor-Dorsey JA, Gredysa DM, et al. A comparison of D2 receptor specific binding in obese and normal-weight individuals using PET with (N-[(11)C]methyl)benperidol. *Synapse* 2013;67:748–756.
26. Brix G, Zaers J, Adam LE, et al. Performance evaluation of a whole-body PET scanner using the NEMA protocol: National Electrical Manufacturers Association. *J Nucl Med* 1997;38:1614–1623.
27. Fischl B. FreeSurfer. *Neuroimage* 2012;62:774–781.
28. Foster ER, Black KJ, Antenor-Dorsey JA, Perlmutter JS, Hershey T. Motor asymmetry and substantia nigra volume are related to spatial delayed response performance in Parkinson disease. *Brain Cogn* 2008;67:1–10.
29. Talairach J, Tournoux P. *Co-planar Stereotaxic Atlas of the Human Brain*. New York: Thieme Verlag; 1988.
30. Hershey T, Black KJ, Carl JL, McGee-Minnich L, Snyder AZ, Perlmutter JS. Long term treatment and disease severity change brain responses to levodopa in Parkinson's disease. *J Neurol Neurosurg Psychiatry* 2003;74:844–851.
31. Logan J, Fowler JS, Volkow ND, Wang GJ, Ding YS, Alexoff DL. Distribution volume ratios without blood sampling from graphical analysis of PET data. *J Cereb Blood Flow Metab* 1996;16:834–840.
32. Hobson AJ, Sterling DA, Emo B, et al. Validity and reliability of an occupational exposure questionnaire for parkinsonism in welders. *J Occup Environ Hyg* 2009;6:324–331.
33. Sanchez G, Determan C. *DiscrimMiner: Tools of the Trade for Discriminant Analysis: R Package Version 0.1–29* [online]. Available at: CRAN.R-project.org/package=DiscrimMiner. Accessed September 15, 2017.
34. Rencher AC, Christensen WF. *Methods of Multivariate Analysis*, 3rd ed. Hoboken: Wiley; 2012.
35. Benjamini Y, Hochberg Y. Controlling the false discovery rate: a practical and powerful approach to multiple testing. *J R Stat Soc Ser B* 1995;57:289–300.
36. Cleveland WS. Robust locally weighted regression and smoothing scatterplots. *J Am Stat Assoc* 1979;74:829–836.
37. Akaike H. Information theory and an extension of the maximum likelihood principle. In: Petrov BN, Csaki F, editors. *Proceedings of the Second International Symposium on Information Theory*. Budapest: Akademiai Kiado; 1973:267–281.
38. Cook RD. Detection of influential observation in linear-regression. *Technometrics* 1977;19:15–18.
39. Criswell SR, Nielsen SS, Warden M, et al. [18F]FDOPA positron emission tomography in manganese-exposed workers. *Neurotoxicology* 2018;64:43–49.
40. Karimi M, Tian L, Brown CA, et al. Validation of nigrostriatal positron emission tomography measures: critical limits. *Ann Neurol* 2013;73:390–396.
41. Brown CA, Karimi MK, Tian L, et al. Validation of midbrain positron emission tomography measures for nigrostriatal neurons in macaques. *Ann Neurol* 2013;74:602–610.
42. Nikolaus S, Antke C, Muller HW. In vivo imaging of synaptic function in the central nervous system, I: movement disorders and dementia. *Behav Brain Res* 2009;204:1–31.
43. Antonini A, Schwarz J, Oertel WH, Pogarell O, Leenders KL. Long-term changes of striatal dopamine D2 receptors in patients with Parkinson's disease: a study with positron emission tomography and [(11)C]raclopride. *Mov Disord* 1997;12:33–38.
44. Antonini A, Vontobel P, Psylla M, et al. Complementary positron emission tomographic studies of the striatal dopaminergic system in Parkinson's disease. *Arch Neurol* 1995;52:1183–1190.
45. Smith Y, Villalba R. Striatal and extrastriatal dopamine in the basal ganglia: an overview of its anatomical organization in normal and Parkinsonian brains. *Mov Disord* 2008;23(suppl 3):S534–S547.
46. Duda J, Potschke C, Liss B. Converging roles of ion channels, calcium, metabolic stress, and activity pattern of Substantia nigra dopaminergic neurons in health and Parkinson's disease. *J Neurochem* 2016;139(suppl 1):156–178.
47. Beaulieu JM, Espinoza S, Gainetdinov RR. Dopamine receptors: IUPHAR review 13. *Br J Pharmacol* 2015;172:1–23.
48. Air Contaminants: Code of Federal Regulations, Title 29, Part 1910.1000, Table Z-1. Washington, DC: US Government Publishing Office; 2011.
49. American Conference of Governmental Industrial Hygienists. *Annual Reports for the Year 2012: Committees on Threshold Limit Values (TLVs) and Biological Exposure Indices (BEIs)*. Cincinnati: ACGIH; 2013.
50. National Institute for Occupational Safety and Health. *Criteria for a recommended standard: welding, brazing, and thermal cutting*. U.S. Department of Health and Human Services, Public Health Service, Centers for Disease Control, National Institute for Occupational Safety and Health, Division of Standards Development and Technology Transfer. Cincinnati: Department of Health and Human Services (National Institute for Occupational Safety and Health); 1988. DHHS (NIOSH) publication No. 88-100.
51. Fitsanakis VA, Zhang N, Garcia S, Aschner M. Manganese (Mn) and iron (Fe): interdependency of transport and regulation. *Neurotox Res* 2010;18:124–131.

Neurology®

Selective D2 receptor PET in manganese-exposed workers

Susan R. Criswell, Mark N. Warden, Susan Searles Nielsen, et al.

Neurology 2018;91:e1022-e1030 Published Online before print August 10, 2018

DOI 10.1212/WNL.0000000000006163

This information is current as of August 10, 2018

Updated Information & Services	including high resolution figures, can be found at: http://n.neurology.org/content/91/11/e1022.full
References	This article cites 43 articles, 11 of which you can access for free at: http://n.neurology.org/content/91/11/e1022.full#ref-list-1
Subspecialty Collections	This article, along with others on similar topics, appears in the following collection(s): Parkinson's disease/Parkinsonism http://n.neurology.org/cgi/collection/parkinsons_disease_parkinsonism PET http://n.neurology.org/cgi/collection/pet Risk factors in epidemiology http://n.neurology.org/cgi/collection/risk_factors_in_epidemiology Screening in epidemiology http://n.neurology.org/cgi/collection/screening_in_epidemiology
Permissions & Licensing	Information about reproducing this article in parts (figures, tables) or in its entirety can be found online at: http://www.neurology.org/about/about_the_journal#permissions
Reprints	Information about ordering reprints can be found online: http://n.neurology.org/subscribers/advertise

Neurology® is the official journal of the American Academy of Neurology. Published continuously since 1951, it is now a weekly with 48 issues per year. Copyright © 2018 American Academy of Neurology. All rights reserved. Print ISSN: 0028-3878. Online ISSN: 1526-632X.

